

## INFLUENCING TRANSITION ON AIRFOILS

D. Althaus  
University of Stuttgart

Presented at the XVIIth OSTIV Congress  
Paderborn, Germany  
May 1981

The performance of airfoils depends primarily on the position and manner of transition from the laminar to the turbulent boundary layer. Independent of the angle of attack or lift coefficient and Reynolds number, these factors define the initial conditions for the turbulent boundary layer. In the range of Reynolds numbers for soaring, between 0.5 and 3.5 million, transition takes place in the separated laminar boundary layer. The turbulent boundary layer then reattaches to the surface and a so-called laminar separation bubble is formed. At higher Reynolds numbers, transition occurs in the boundary layer attached to the wall. Thus, initial conditions for the turbulent boundary layer can be quite different. Depending on the form of the pressure rise for the turbulent boundary layer, a variation of the initial conditions can imply early separation of the boundary layer. In designing an airfoil, proper handling of boundary layer transition at all flight conditions is a primary aim. Figure 1 shows the velocity distribution for the Liebeck R 1511 airfoil. This is an example of an airfoil without any provision for influencing boundary layer transition. The stable laminar boundary layer suddenly must sustain the sharp turbulent pressure rise. Oil flow pictures, taken during wing tunnel tests, showed a laminar separation bubble with a length of 30% of chord forming at the beginning of the pressure rise. By means of a trip wire, position at  $x/c = 0.3$ , the instability of the laminar boundary layer was increased, resulting in a rather small separation bubble. The drag could be appreciably

reduced as is demonstrated in Figure 2. This example shows that handling of transition is essential. Methods for controlling transition will be demonstrated.

Transition can be achieved by shaping of the contour. F.X. Wortmann<sup>1</sup> shows that it is possible to control transition by inserting a so-called instability range with a flat negative velocity gradient between the positive and the negative velocity gradients. The velocity distributions of the 13% thick airfoil WP 2 at an angle of attack of  $\alpha = 1.3^\circ$ , shown in Figure 3, have no instability ranges. Wind tunnel tests revealed laminar separation bubbles at the beginning of the pressure rise as marked in the Figure. The velocity distribution of the upper side was modified with an instability range beginning at 30% of chord developing a laminar boundary layer with constant form parameter. This velocity distribution is shown on the Figure by the broken line called WP 2 MOD. The contour of the wind tunnel model WP 2 was modified accordingly. At a chord length of 500 mm, the change in contour had a maximum length of 1 mm. The drag polars for the original model WP 2 and the modified model WP 2 MOD are shown in Figure 4. The polar of the WP 2 airfoil for  $Re = 0.7$  million, shows the form of the laminar drag bucket characteristic of laminar separation bubbles. By the application of the instability range on airfoil WP 2 MOD, the drag is maintained constant within the whole laminar bucket. At higher Reynolds numbers, the reduction in drag by incorporation of the instability range is small, as is to be expected; at the upper end of the

laminar bucket the drag even increases. This is no disadvantage since on an airfoil in flight, at high Reynolds numbers, only the medium and low range of the laminar bucket is used.

Another example of the use of the instability range is shown in Figure 5. The symmetrical airfoil IS 30 A/150 with a thickness of 15% is designed with an instability range from 40-70% of chord. A new instability range beginning at about 45%, with a somewhat higher form parameter and a resulting stronger pressure gradient, was calculated. The shape of the upper side of the wind tunnel model was modified accordingly. Figure 6 shows the drag polars for the symmetrical airfoil and the airfoil IS 30 A/150 MOD with modified upper side. A small reduction in drag was achieved at negative angles of attack for small Reynolds numbers. At high Reynolds numbers and positive angles of attack, the drag coefficient is increased, i.e. the pressure gradient in the instability range is too high and transition occurs too early in the instability region.

Distinct disturbances on the surface of the airfoil reveal a further possibility for controlling transition; they also increase the instability of the laminar boundary layer. Roughnesses, as once used, are difficult to produce and to fix at the airfoil surface. The installation of trip wires is also problematic. Neither device is suited for use on an airplane. The author uses transition trips consisting of self-sticking Mylar film with pressed in bumps of a spherical or grain-like form. Strips of any width are easily produced with a modified sewing machine. The needle is replaced by one with a ball-shaped tip. The height of the bumps and their distance can be varied. These transition trips are easily reproduceable and can be installed anywhere on an airfoil surface. Recently, blowing of air has again been claimed to be a favorable transition device. Small amounts of air are blown through small holes perpendicular to the airfoil surface. The disadvantage of this method is the laborious and expensive installation of the holes and the air supply. The holes

can be obstructed by dirt and rain. The only advantage of this installation may be that blowing can be turned off when it is not needed. But this is difficult to achieve because circulation of air induced by the spanwise pressure gradients must be avoided.

As examples of the application of transition devices, the drag polars for the airfoil WP 2 are shown in Figure 7. On this airfoil, no instability range is provided (see Figure 3). Strips with sand-grain roughness were installed on the upper side between 60 and 62% of chord, and on the lower side between 72 and 74%, i.e. at the beginning of the pressure rise or the laminar separation bubble. At smaller Reynolds numbers, the drag is reduced, but at the higher Reynolds numbers drag penalties have to be allowed for. Position and height of the roughness was not optimized in this case. For clarity, the origin of the curves for the different Reynolds numbers have been shifted in Figure 7.

Figure 8 demonstrates drag polars for a flapped airfoil at a Reynolds number of 2 million. At a flap setting of  $\beta = -5^\circ$ , an appreciable drag reduction could be achieved with a Mylar film tripping device (as mentioned above) on the lower surface of the airfoil at 80% of chord, i.e. just ahead of the hinge of the flap. The velocity distribution in Figure 9 reveals a sharp transition to the turbulent pressure rise at the hinge of the flap, resulting in a laminar separation bubble. With the transition trip, this bubble is minimized and thereby the drag reduced.

Figure 10 shows a drag polar for the flapped airfoil HQ 19/1398 at a Reynolds number of 2.5 million and a flap setting of  $\beta = -10^\circ$ . The wind tunnel model was fitted with the blowing installation mentioned above. The broken line pertains to a measurement with the holes sealed by a thin film. By blowing a small amount of air, reduction in drag could be achieved as shown by a full line. Exactly the same polar was attained when the holes were sealed by a thin film having a bump with a height of 0.5 mm over each hole. This device is of course cheaper and simpler than the complicated installation for blowing. The velocity distribution for

this airfoil looks like that shown in Figure 9. By blowing air or by triggering transition through roughness, boundary transition was forced at the hinge of the flap, resulting in a small laminar separation bubble.

Triggering transition by blowing or by disturbances at the surface can be successfully applied where thick and long laminar separation bubbles have to be diminished or removed. Large separation bubbles form when a relatively stable laminar boundary layer must sustain an abrupt transition to a sharp pressure rise. This is the case on airfoils with long laminar runs, or on airfoils designed for high lift which have high super velocities on the upper surface. To reach the trailing edge velocity with a tolerable pressure gradient for the turbulent boundary layer, the recovery has to begin rather early.

On airfoils with velocity distributions showing a mild pressure rise within the laminar range, or some sort of instability range, only small laminar separation bubbles are formed. Experience shows that a reduction in drag is difficult to achieve by disturbances on the surface or blowing in this case. Either there is no effect or the drag may even increase. A proper instability range in the velocity distribution provided in the design of the airfoil will be preferable.

Boundary layer transition can be affected by an unwanted tripping device: insects! During the summer, insects are collected on the airfoil nose and form roughnesses for the laminar boundary layer. From each roughness, if high enough, a wedge-shaped turbulent boundary layer emerges. After a short distance, these wedges form a uniform turbulent boundary layer along the span of the wing. This early transition results in an increase of drag. At the beginning of the pressure rise, there is now a thick turbulent boundary layer which will separate early. This results in a reduction of the lift coefficient.

Calculations of the performance of airplanes are often based on the assumption of ideal smooth airfoils. What losses in performance have to be expected from roughness due to insects?

Johnson<sup>3</sup> made flight tests on sailplanes with artificial insects. He used small pieces of tape with a length of 5 x 5 mm and a height of 0.25 mm. A row of these "bugs" was fixed on the airfoil nose in a distance of 150 mm. Some 12 mm above and below the airfoil nose, further rows of bugs were fixed in an alternating pattern. Thus, 1 m of span was fitted with 20 bugs. This surely does not correspond to reality, but some standard was defined.

To perform comparable wind tunnel tests on airfoils with insects, a pattern for insects on airfoil noses was established. 10 mm wide strips of Mylar film, 0.2 mm thick, with bumps at a distance of 30 mm and 0.5 mm high, are used. One of these strips is fastened on the airfoil nose in such a way that the bumps are directly on the nose line. One strip is fixed on the lower side and two further strips on the upper side of the airfoil nose, in such a way that the bumps are shifted spanwise half the distance from strip to strip. This results in about 130 bugs per meter span. This pattern is thought to conform to reality. The advantage of this method is that the strips are easy to produce and to mount, and the pattern is easily reproduceable.

Tests on airfoils with this bug pattern provide information about the sensitivity of particular airfoils with equal disturbances. Figure 11 shows the drag polars of the airfoil FX 61-163 with artificial insects, according to the pattern described above. Results for the clean airfoil are drawn as dashed lines for comparison. In the upper range of the low drag bucket, an increase in drag results from the bugs. At lower lift coefficients, the increase in drag is larger for  $Re = 2.5$  million than for  $Re = 1$  million. As Figure 12 shows, the influence of roughness due to insects is even more drastic on airfoils with flaps. Tests on the airfoil FX 67-K-150/17 are shown in Figure 12 as an example. In comparison to the results on the clean airfoil, substantial deficiencies are shown in the lower range of the bucket. The results are even worse on the upper end of the bucket. The slope of the lift curve has flattened compared with the clean

airfoil results, although the maximum lift is nearly the same for both cases. Tests on the airfoil FX 62-K-131/17 in Figure 13 show similar results for  $Re = 1$  million. At  $Re = 2.5$  million the increase in drag is somewhat smaller than in the former example. In the upper range of the bucket, the drag is smaller for  $Re = 2.5$  million than for  $Re = 1$  million.

The losses due to insect roughness are smaller for the unflapped airfoil FX 61-163 than for the flapped ones. The pressure rises for the airfoil FX 61-163 on both sides are flatter than those for flapped airfoils at positive or at negative flap settings. If, owing to the roughness due to insects, transition is forced near the airfoil nose, the turbulent boundary layer at the beginning of the pressure rise is thicker than for the clean airfoil. Flapped airfoils show premature separation for this reason.

Performance of sailplanes with these airfoil-bug-polars: two 15 m span sailplanes were evaluated with the airfoil polars in Figures 11 and 12. Figure 14 shows the polar for straight flight and circling for a 15 m FAI sailplane with a clean wing and wing with bugs, with the flapped airfoil FX 67-K-150/17. Figure 15 demonstrates the polars for a 15 m standard sailplane with the airfoil FX 61-163. In Table 1, some figures from these performance calculations are collected. In addition, the relative penalties caused by the insects are demonstrated. The losses in performance are larger for the flapped airplane. These calculated penalties are somewhat larger than those measured by Johnson owing to his rather crude bug pattern.

In the wind tunnel tests, all airfoils were tested with the same bug pattern. However, from experience we know that different airfoils collect different numbers of bugs under similar conditions. The impingement and rupture of insects depends on the shape of the airfoil nose, the position of the stagnation point, and the airfoil

thickness. Essential factors for the rupture of the insects are the velocity and the angle of impingement.

In order to get more information about the vulnerability of different airfoils to insect impact, some information should be gathered by evaluating the bug pattern on wings after flight. A thin Mylar film could be affixed to the wing leading edge. When the airfoil nose line is marked on the film, the distribution of insects can easily be evaluated when the film is detached after the flight. The film with the bugs could even be fixed on a wind tunnel model of the same airfoil to get wind tunnel results with the real pattern.

These tests and examples show the detrimental losses in performance caused by the contamination of insects. The airfoils designed for high performance turn out to be the most vulnerable ones. Perhaps some relaxation of performance of the clean airfoil, thereby resulting in a smaller loss to insects, would be a compromise. F.X. Wortmann<sup>4</sup> showed in 1963 that contamination by insects can be avoided by the use of an elastic airfoil nose. The high expense of an airplane with high performance makes it desirable to look for a way to guarantee this performance to a certain degree, even with roughness due to insects.

#### REFERENCES

1. F.X. Wortmann, "Experimentelle Untersuchungen an neuen Laminarprofilen für Segelflugzeuge und Hubschrauber," ZfW 5, 1957.
2. F.X. Wortmann, "Boundary Layer and Flow Control," Pergamon-Press, 1961.
3. R. Johnson, "Flight Test Evaluations," Soaring, Soaring Society of America.
4. F.X. Wortmann, "Über eine Möglichkeit zur Vermeidung der Insektenrauhigkeit," 9. OSTIV-Kongress, 1963, Argentinien, Schweizer Aero-Revue 11, 1963.

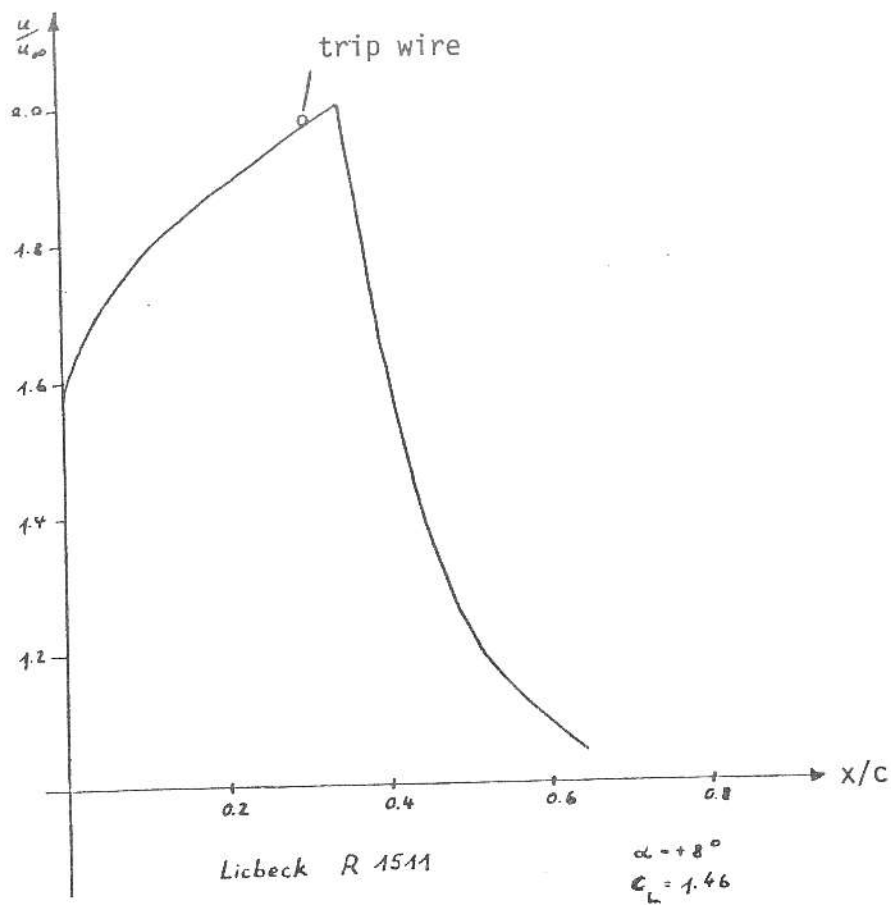


Fig. 1

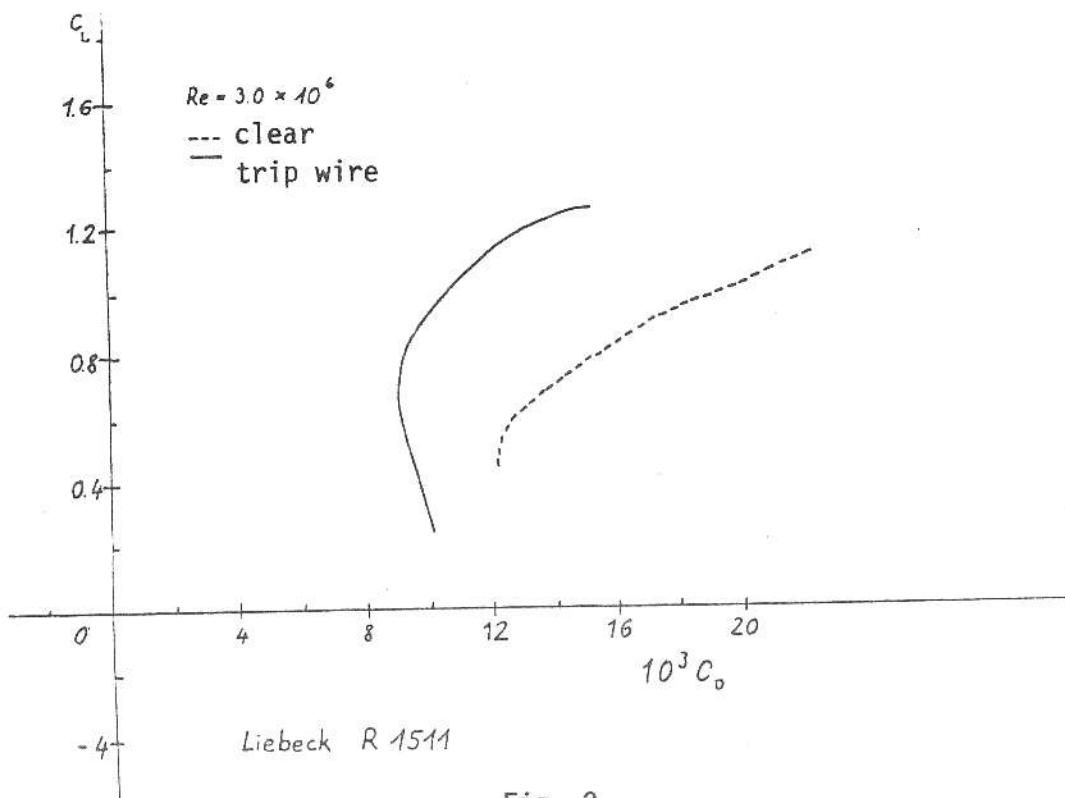


Fig. 2

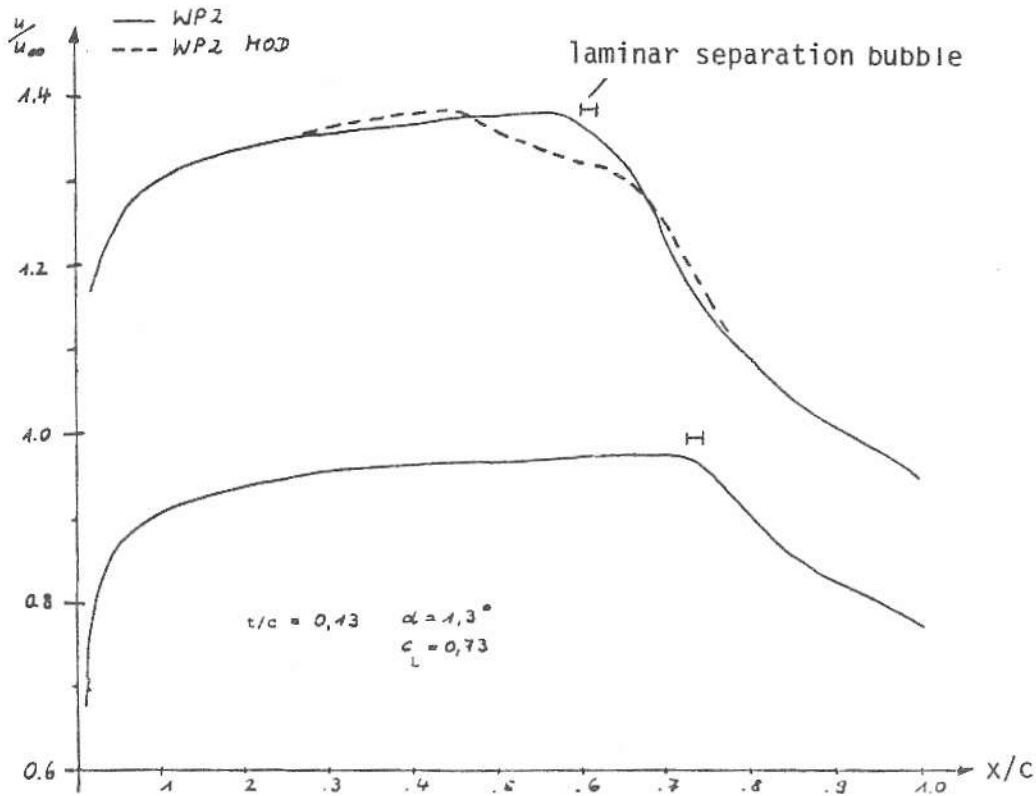


Fig. 3

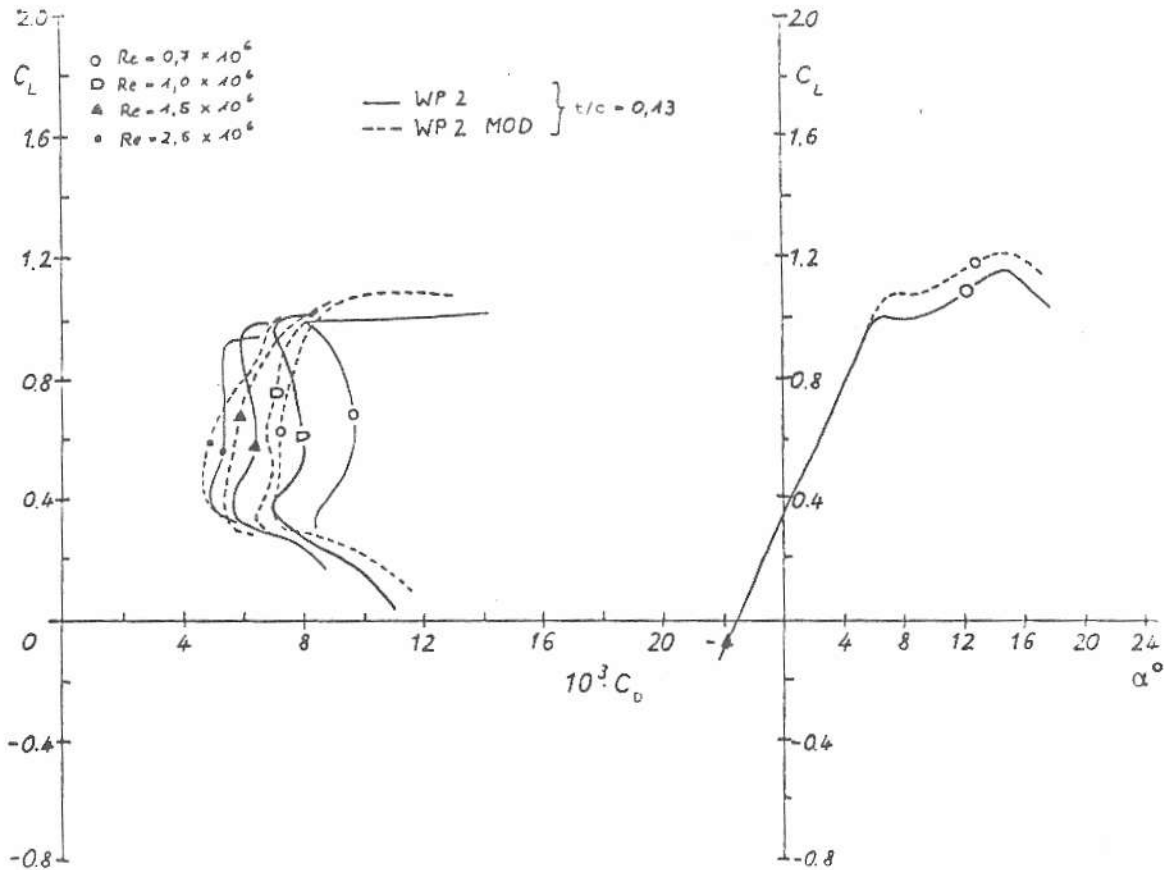


Fig. 4

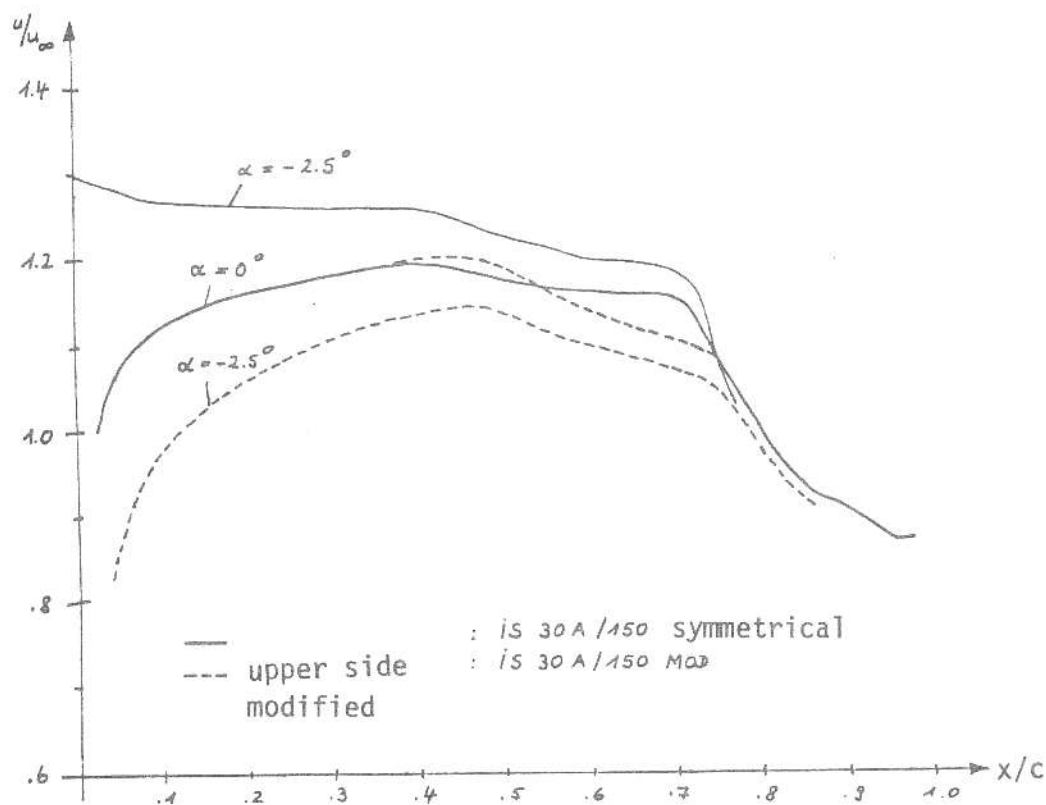


Fig. 5

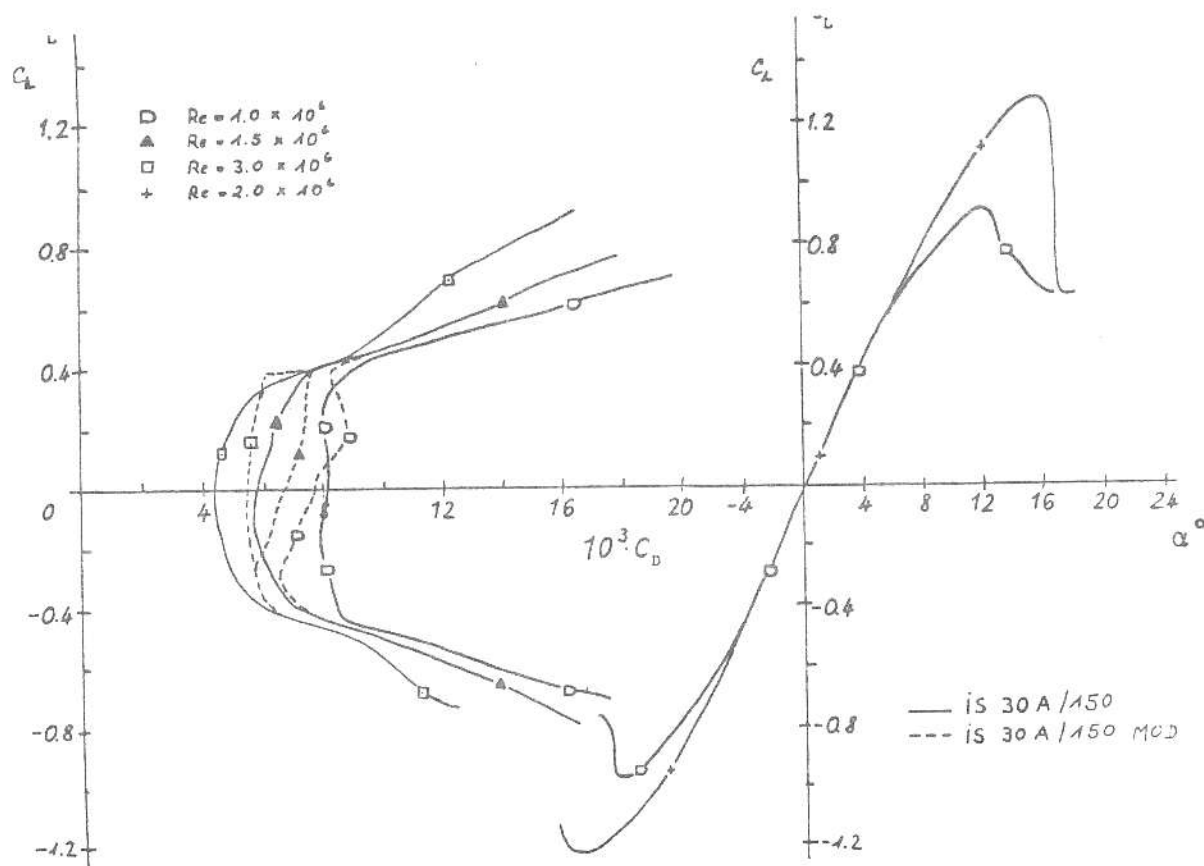


Fig. 6

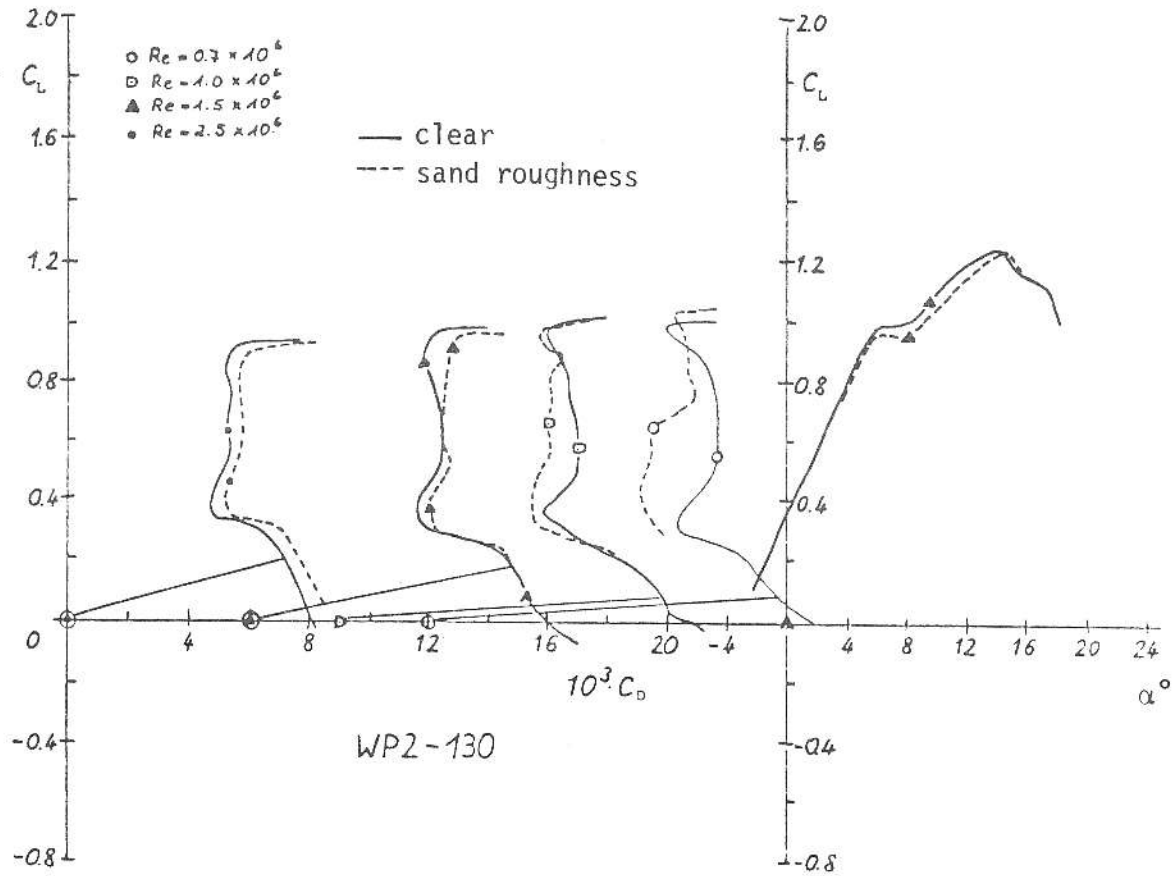


Fig. 7

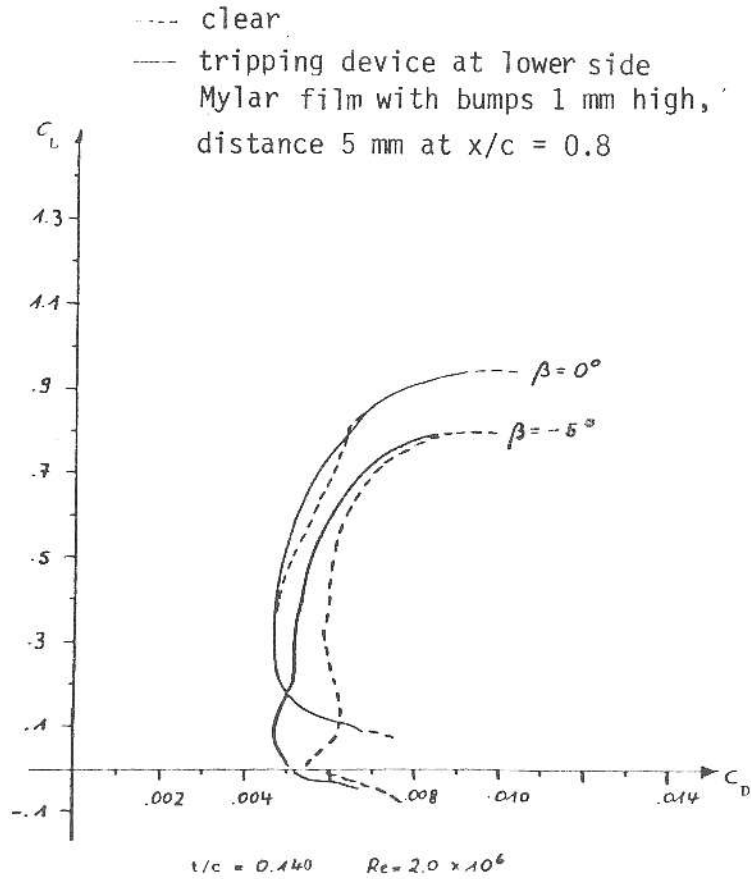


Fig. 8

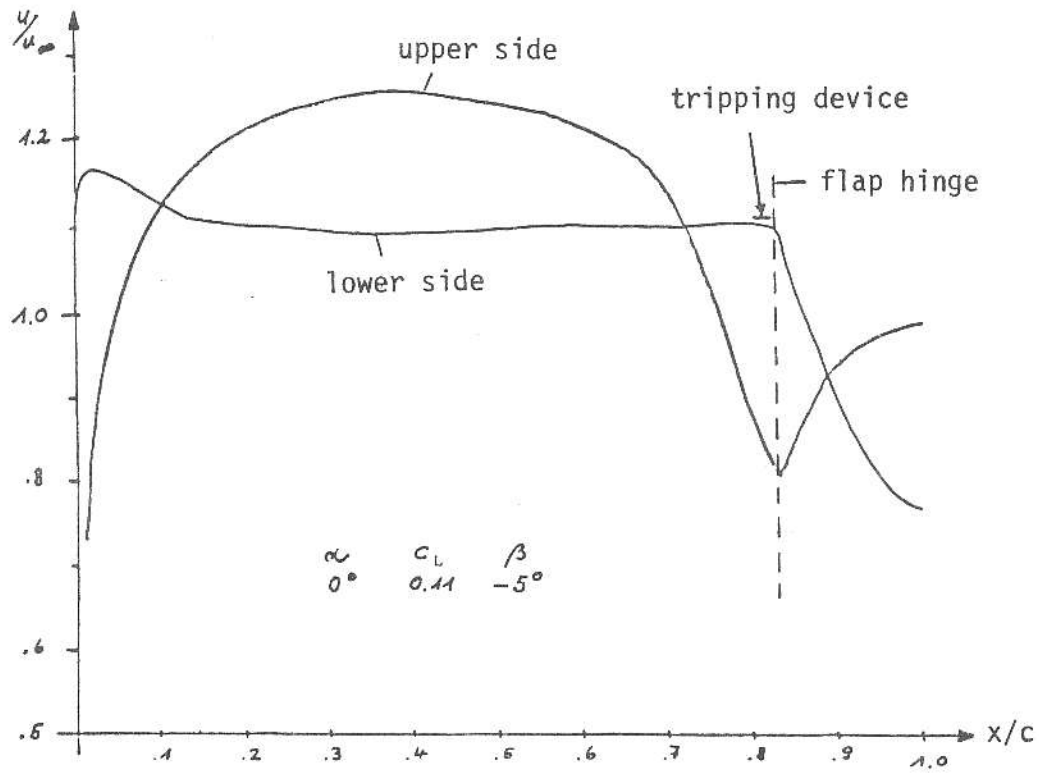


Fig. 9

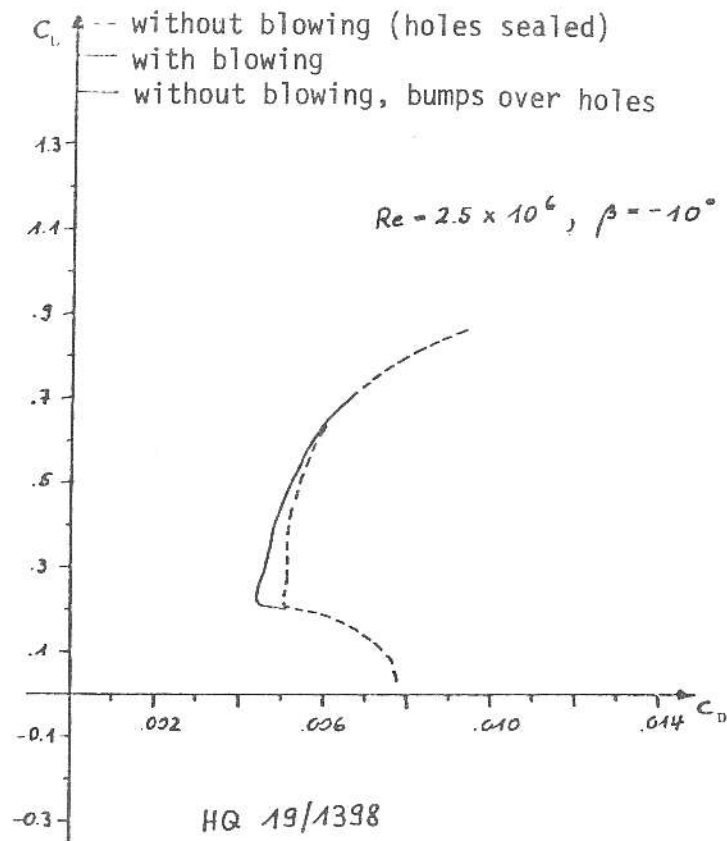


Fig. 10

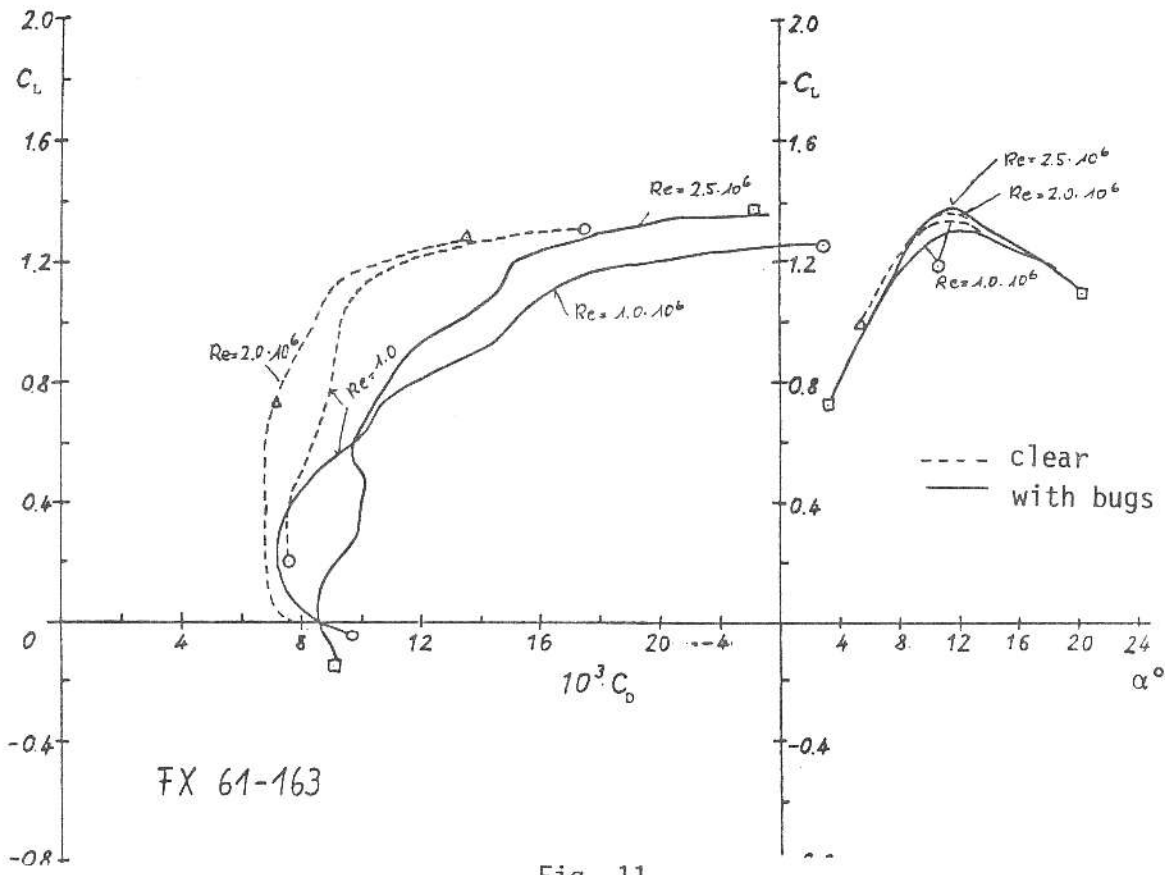


Fig. 11

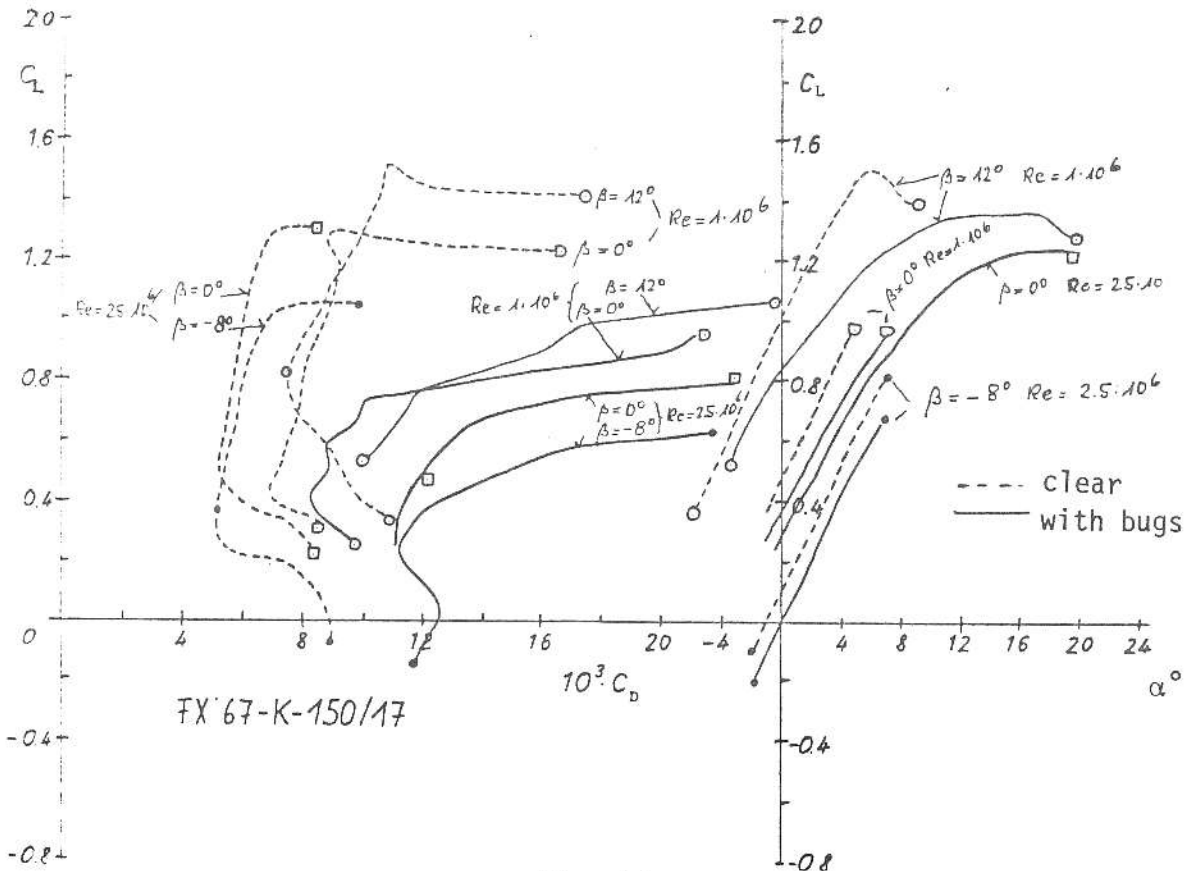


Fig. 12

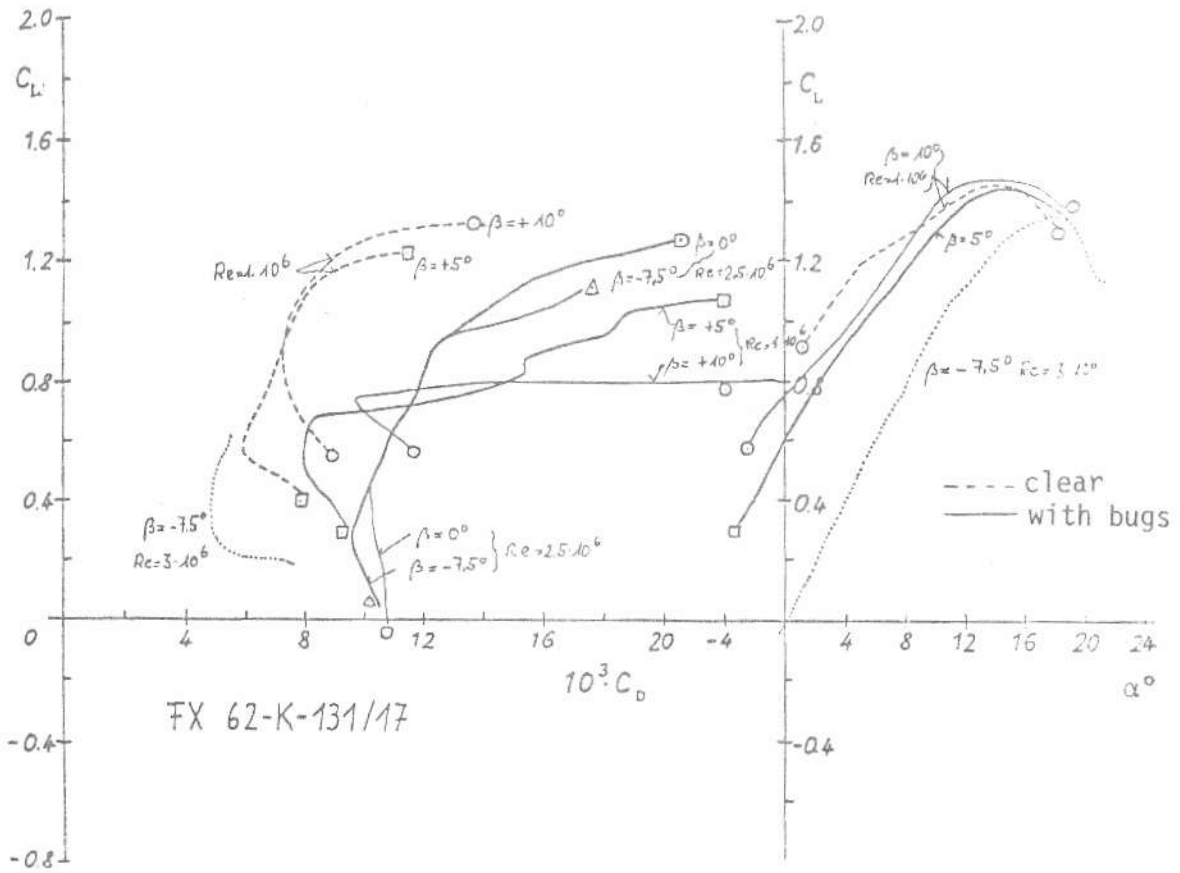


Fig. 13

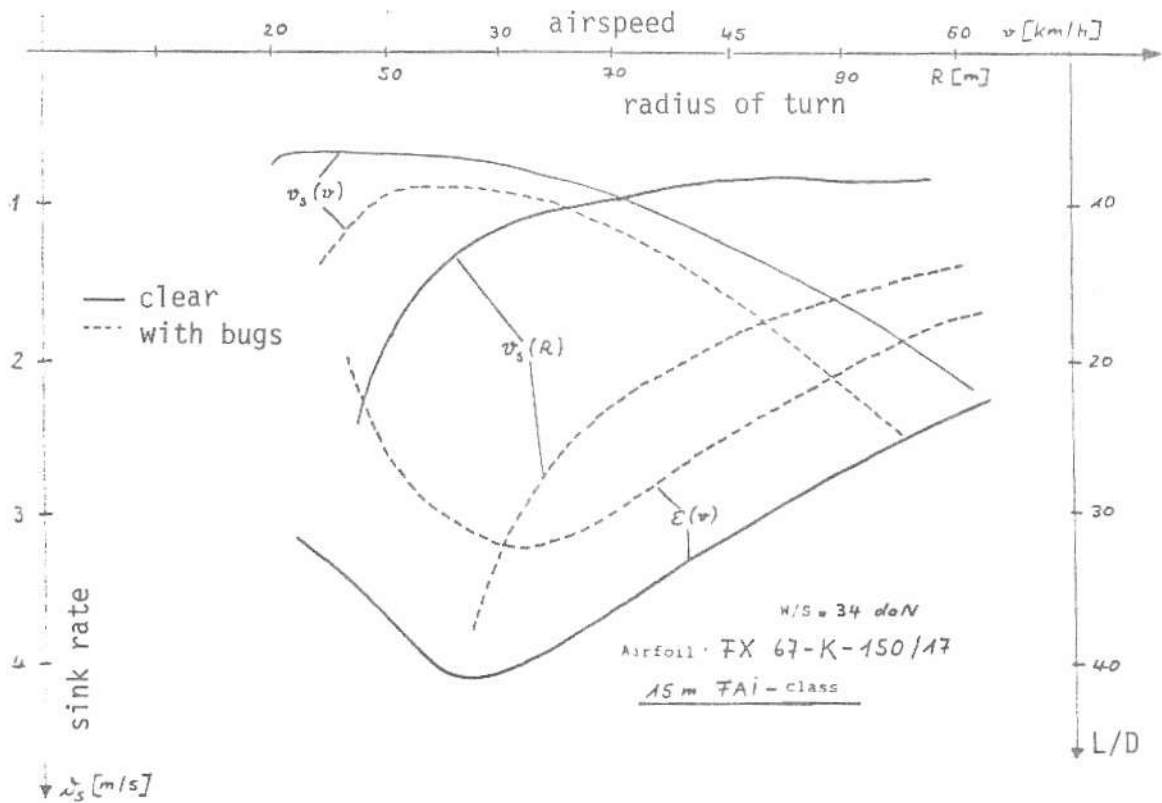


Fig. 14 The influence of bugs on calculated polars for straight and circling flight

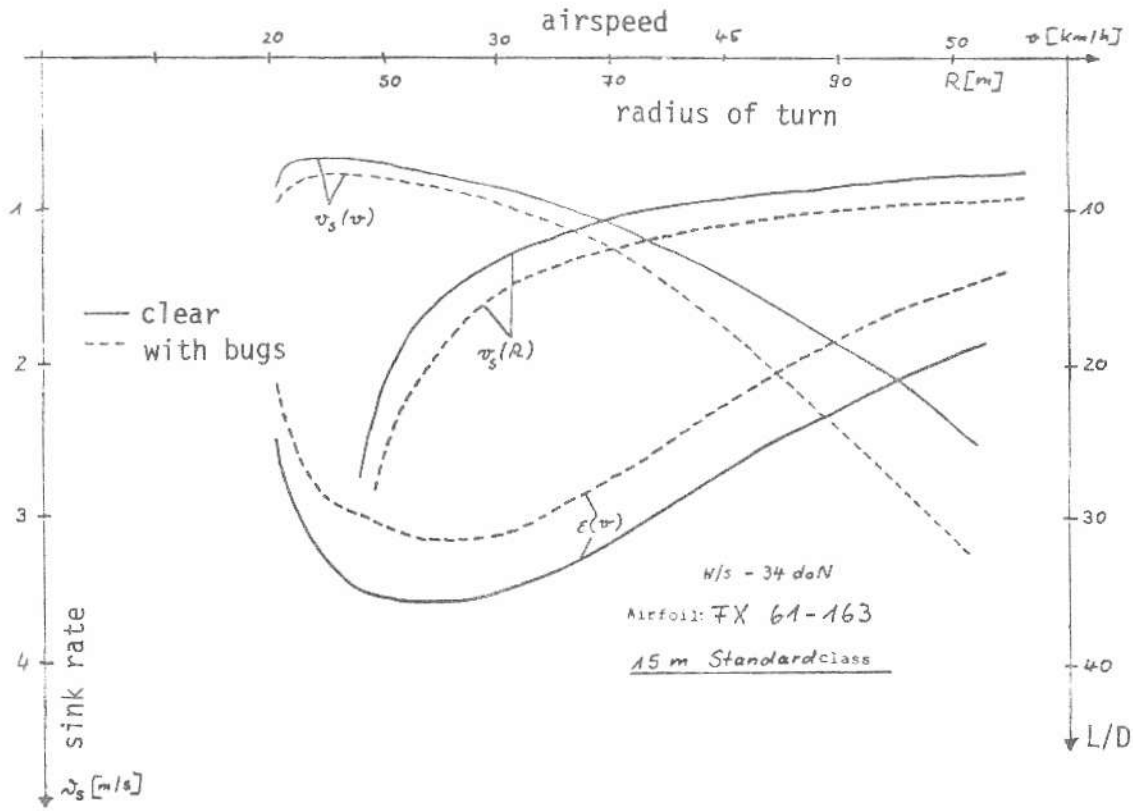


Fig. 15 The influence of bugs on calculated polars for straight and circling flight

| $W/s = 34 \text{ daN/m}^2$                                    | 15 m FAI - class<br>FX 67-K-150/17 |      |      | 15 m Standard class<br>FX 61-163 |      |     |
|---|------------------------------------|------|------|----------------------------------|------|-----|
|   | clear                              | bugs | %    | clear                            | bugs | %   |
| min. sink rate<br>$v_{S \text{ min}}$ [m/s]                   | 0,66                               | 0,94 | +38  | 0,67                             | 0,78 | +16 |
| opt. L/D<br>$E_{\text{opt}}$                                  | 40,9                               | 32,0 | -22  | 35,8                             | 32,0 | -11 |
| sink rate [m/s] at<br>110 [km/h]                              | 0,75                               | 0,94 | +25  | 0,86                             | 1,0  | +16 |
| sink rate [m/s] at<br>185 [km/h]                              | 2,3                                | 2,87 | +25  | 2,6                              | 3,37 | +29 |
| sink rate [m/s] at<br>Radius 55 [m]                           | 1,37                               | 4,8  | +250 | 1,57                             | 1,89 | +20 |
| sink rate [m/s] at<br>Radius 75 [m]                           | 0,89                               | 2,06 | +131 | 0,98                             | 1,17 | +19 |
| Radius of turn [m]<br>at 1,5 [m/s] sinkrate                   | 52                                 | 90   | +73  | 55                               | 62   | +13 |
| cross country speed<br>for a climb rate<br>at 2 m/s<br>[km/h] | 86                                 | 72   | -16  | 82                               | 76   | -7  |

The influence of bugs on calculated performance of sailplanes

Table 1